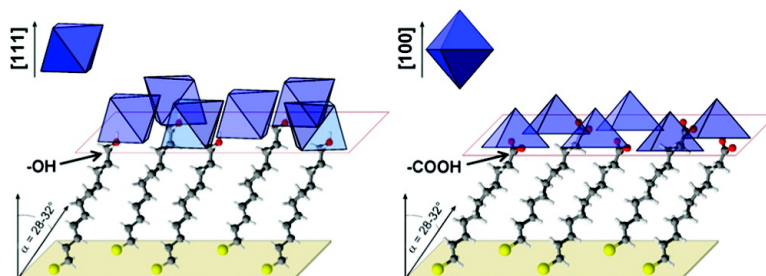


Oriented Growth of the Metal Organic Framework Cu(BTC)(HO) \cdot xHO Tunable with Functionalized Self-Assembled Monolayers

Enrica Biemmi, Camilla Scherb, and Thomas Bein

J. Am. Chem. Soc., **2007**, 129 (26), 8054-8055 • DOI: 10.1021/ja0701208 • Publication Date (Web): 07 June 2007

Downloaded from <http://pubs.acs.org> on February 16, 2009



More About This Article

Additional resources and features associated with this article are available within the HTML version:

- Supporting Information
- Links to the 21 articles that cite this article, as of the time of this article download
- Access to high resolution figures
- Links to articles and content related to this article
- Copyright permission to reproduce figures and/or text from this article

[View the Full Text HTML](#)

Oriented Growth of the Metal Organic Framework $\text{Cu}_3(\text{BTC})_2(\text{H}_2\text{O})_3 \cdot x\text{H}_2\text{O}$ Tunable with Functionalized Self-Assembled Monolayers

Enrica Biemmi, Camilla Scherb, and Thomas Bein*

Department of Chemistry and Biochemistry, University of Munich, Butenandtstr. 5-13 (E), D-81377 Munich, Germany

Received January 7, 2007; E-mail: bein@lmu.de

Here we report the tunable, oriented growth of the porous framework HKUST-1,¹ ($\text{Cu}_3(\text{C}_9\text{H}_3\text{O}_6)_2(\text{H}_2\text{O})_3 \cdot x\text{H}_2\text{O}$, abbreviated $\text{Cu}_3(\text{BTC})_2$), on different functionalized self-assembled monolayers (SAMs). The chemistry of metal organic frameworks (MOFs) has been intensively studied, with particular attention to porous compounds due to their many potential applications such as gas sorption, molecular separation, storage, and catalysis.² To date, the research efforts have been mainly focused on bulk materials; the preparation of thin films of those compounds is an important challenge. The growth of one MOF structure, such as MOF-5, has been reported on a SAM of COOH-terminated alkanethiols; however, this film did not show preferred crystal orientation.³

The ability to control the orientation of the crystals and thus the pore system in such films will open the way to more advanced applications such as selective gas separation membranes or chemical sensors. The successful oriented growth of inorganic compounds, such as calcium carbonate,⁴ lead sulfide,⁵ anatase,⁶ zinc and iron oxide,^{7,8} and zeolites,^{9,10} on functionalized surfaces has inspired us to explore the effect of self-assembled monolayers¹¹ with different functionalities on the growth of $\text{Cu}_3(\text{BTC})_2$. Its structural features and stability as well as its intriguing sorption and catalytic properties^{12–14} make this material an interesting candidate for the growth of thin films.

In many metal organic frameworks, such as MOF-5, the coordination sites of the metal ions are blocked by the ligands serving as connectors in the network. In contrast, the Cu^{2+} ions in $\text{Cu}_3(\text{BTC})_2$ present available coordination sites on the axial direction of the “paddle-wheel” Cu_2 cluster (Figure S1), which are occupied by weakly bound water molecules.¹² In the present study, these accessible coordination sites are viewed as potential binding sites for the functional groups terminating different SAMs.

For the growth of the $\text{Cu}_3(\text{BTC})_2$ crystals, gold substrates were modified with monolayers of $\text{HS}(\text{CH}_2)_{10}\text{X}$ (with $\text{X} = \text{CO}_2\text{H}$, $\text{CH}_2\text{-OH}$, CH_3) following known procedures.^{15,16} The carboxylic acid functionality imitates the organic linker (1,3,5-benzenetricarboxylate (BTC)) in the open framework structure, the alcohol group mimics the coordinating water, and the methyl group presents an inert reference surface. On the basis of this reasoning, we anticipated different orientations of the crystals on the $-\text{CO}_2\text{H}$ - and $-\text{OH}$ -functionalized SAMs, considering the fundamental differences in the coordination geometry in the structure.

Thin films of $\text{Cu}_3(\text{BTC})_2$ crystals were obtained on each modified gold surface. No crystallization takes place on bare gold surfaces. After SAM formation, the gold-coated slides ($1 \times 1.3 \text{ cm}^2$) were placed face-down on Teflon supports in a clear $\text{Cu}_3(\text{BTC})_2$ crystallization solution and left at room temperature for different periods of time (8–210 h). The crystallization solution is obtained by filtration of a typical HKUST-1 synthesis mixture left for 8 days at 75°C (Scheme S1).

Highly ordered thin films of $\text{Cu}_3(\text{BTC})_2$ were formed on the SAMs as demonstrated by the diffraction patterns shown in Figure

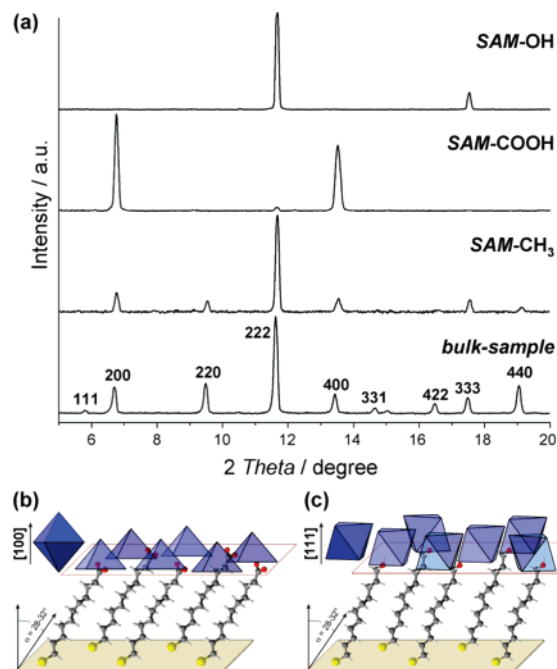


Figure 1. (a) X-ray diffraction patterns (background corrected) of thin films of $\text{Cu}_3(\text{BTC})_2$ on functionalized gold surfaces, compared with a randomly oriented $\text{Cu}_3(\text{BTC})_2$ powder sample measurement. Each pattern is normalized to the most intensive reflection. Bottom: Schematic illustrations of oriented growth of HKUST-1 nanocrystals controlled via surface functionalization: (b) on an 11-mercaptoundecanoic acid SAM, and (c) on 11-mercaptoundecanol-modified gold surfaces. The alkanethiol self-assembled monolayers are represented with a tilt of ca. 30° from surface normal as reported in the literature.¹⁶

1a. The film grown on the $-\text{COOH}$ self-assembled monolayer is highly oriented along the [100] direction, while the OH-modified surface induces a completely different orientation along the [111] direction. Homogeneous but less oriented thin films are also obtained on the methyl SAM. Figure 1b,c shows a schematic illustration of the surface-induced oriented growth of $\text{Cu}_3(\text{BTC})_2$ crystals. To our knowledge, this is the first demonstration of complete molecular control of the growth orientation of metal organic frameworks.

We propose that the two different termini ($-\text{COOH}$ and $-\text{OH}$) of the SAMs force the oriented attachment of appropriate growth species at the molecular interface, followed by oriented crystal growth on the molecular layer on the substrate.

The temporal evolution of the growth process was followed in order to learn more about the mechanism of formation of the thin films on each modified surface ($-\text{OH}$ -, $-\text{COOH}$ -, and $-\text{CH}_3$ -terminated SAMs). The samples were removed from the crystallization solution after different immersion times, dried at room temperature, and characterized. Figure 2a shows the evolution of

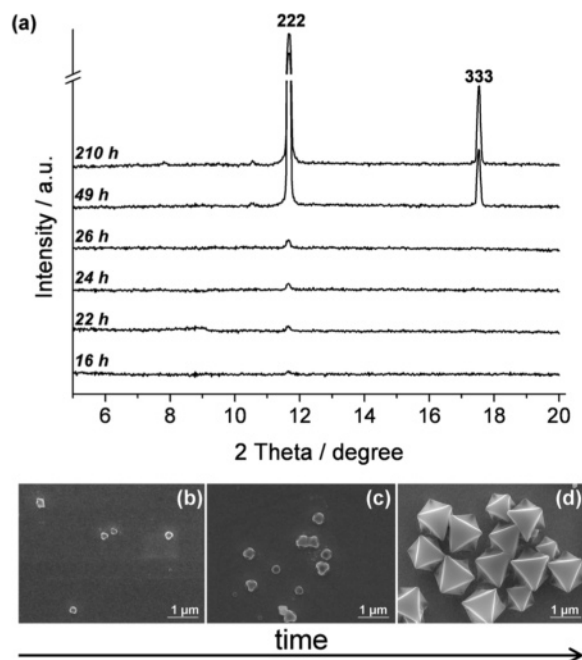


Figure 2. (a) Diffraction patterns of [111]-oriented $\text{Cu}_3(\text{BTC})_2$ crystals on OH SAMs collected after immersion times between 16 and 210 h. Related scanning electron micrographs of face-down samples after immersion in the crystallization solution for (b) 16, (c) 24, and (d) 45 h.

the diffraction patterns of [111]-oriented $\text{Cu}_3(\text{BTC})_2$ crystals on OH SAM, collected after immersion times between 16 and 210 h. The intensity of the reflections increases with the reaction time because of both the number and the size of the crystals on the surface increase. The scanning electron micrographs presented in Figure 2b–d show, in detail, the morphological development of the crystals from “rounded” octahedra of 150–200 nm in diameter at the first stages (Figure 2b) up to 1 μm well-shaped crystals after 45 h (Figure 2d).

An analogous investigation was performed on the COOH- and CH_3 -functionalized samples. Figure S3a (see Supporting Information) shows the diffraction patterns of the gold slides modified with the carboxylic acid SAM. After about 62 h, the (200) and (400) reflections of the $\text{Cu}_3(\text{BTC})_2$ crystals appear, followed by further growth until the end of the experiment (112 h). With the exception of a minute (222) peak, the (200) and (400) reflections completely dominate the pattern, thus demonstrating the growth of a highly oriented crystalline film of $\text{Cu}_3(\text{BTC})_2$. A close look at the morphology of the film after 40 h (Figure S4) reveals that already after 40 h in solution many small [100] oriented crystals can be detected “growing out” of the SAM gold substrate, in addition to a few [111]-oriented crystals which cause the minute additional (222) reflection.

The Cu_3BTC_2 crystal layer on the methyl-terminated SAM shows a faster growth process than on the other two polar layers, with no unique orientation (as shown in the SEM pictures presented in Figures S5). The X-ray diffraction patterns present all typical reflections of $\text{Cu}_3(\text{BTC})_2$, while the (222) reflection is predominant (Figure S3b). Thus the [111] direction appears to be favored for less selective crystal growth; we propose that, in this case, the growth species have already assumed an octahedral shape with

{111} faces that can attach to the surface. This should constitute a favorable attachment mechanism if dispersive forces between the organically terminated crystal faces and the alkyl-terminated SAM are dominant. After long immersion times (>100 h), ca. 600 nm thin films composed of a monolayer of close-packed intergrown crystals were found on all functionalized gold substrates (Figure S6).

The above results clearly demonstrate that different molecular functionalities of the self-assembled monolayers induce different, well-defined orientations of the $\text{Cu}_3(\text{BTC})_2$ crystals grown on gold. Although the mechanism of this remarkable effect is still unknown, a reasonable model could invoke selective interactions of crystal building blocks in solution with the functionalized surfaces. The thermal pretreatment of the synthesis solution (8 days at 75 $^\circ\text{C}$) induces the crystallization process; after filtration of the solid product, we anticipate the existence of colloidal or molecular building blocks of $\text{Cu}_3(\text{BTC})_2$ in the solution. Taking into account the paddle-wheel motif in the open framework structure, different coordination modes of the carboxylic or the alcoholic groups might control the selective nucleation on the substrate, thus mimicking either axial (as with water) coordination with the alcohol terminus or chelating coordination (as with BTC) with the $-\text{COOH}$ terminus of the SAM, respectively.

Acknowledgment. The authors would like to thank Dr. Ralf Köhn for fruitful discussions, and Dr. Steffen Schmidt and Andreas Zürner for help in the sample characterization.

Supporting Information Available: Detailed synthesis procedure, RAIR spectra of the SAM-modified gold surfaces, and XRD patterns and SEM images of the thin films. This material is available free of charge via the Internet at <http://pubs.acs.org>.

References

- Chui, S. S. Y.; Lo, S. M. F.; Charmant, J. P. H.; Orpen, A. G.; Williams, I. D. *Science* **1999**, *283*, 1148–1150.
- (a) Ockwig, N. W.; Delgado-Friedrichs, O.; O’Keeffe, M.; Yaghi, O. M. *Acc. Chem. Res.* **2005**, *38*, 176–182. (b) Surlbe, S.; Millange, F.; Serre, C.; Duren, T.; Latroche, M.; Bourrelly, S.; Llewellyn, P. L.; Férey, G. *J. Am. Chem. Soc.* **2006**, *128*, 14889–14896. (c) Férey, G.; Mellot-Draznieks, C.; Serre, C.; Millange, F.; Dutour, J.; Surlbe, S.; Margiolaki, I. *Science* **2005**, *309*, 2040–2042. (d) Kitagawa, S.; Kitaura, R.; Noro, S.-J. *Angew. Chem., Int. Ed.* **2004**, *43*, 2338–2375.
- Hermes, S.; Schroeder, F.; Chelmoski, R.; Woell, C.; Fischer, R. A. *J. Am. Chem. Soc.* **2005**, *127*, 13744–13745.
- Aizenberg, J.; Black, A. J.; Whitesides, G. M. *J. Am. Chem. Soc.* **1999**, *121*, 4500–4509.
- Meldrum, F. C.; Flath, J.; Knoll, W. *J. Mater. Chem.* **1999**, *9*, 711–723.
- Wang, D.; Liu, J.; Huo, Q.; Nie, Z.; Lu, W.; Williford, R. E.; Jiang, Y.-B. *J. Am. Chem. Soc.* **2006**, *128*, 13670–13671.
- Hsu, J. W. P.; Tian, Z. R.; Simmons, N. C.; Matzke, C. M.; Voigt, J. A.; Liu, J. *Nano Lett.* **2005**, *5*, 83–86.
- Bunker, B. C.; Rieke, P. C.; Tarasevich, B. J.; Campbell, A. A.; Fryxell, G. E.; Graff, G. L.; Song, L.; Liu, J.; Virden, J. W.; McVay, G. L. *Science* **1994**, *264*, 48–55.
- Feng, S.; Bein, T. *Nature* **1994**, *368*, 834–836.
- Lee, J. S.; Lee, Y.-J.; Tae, E. L.; Park, Y. S.; Yoon, K. B. *Science* **2003**, *301*, 818–821.
- Love, J. C.; Estroff, L. A.; Kriebel, J. K.; Nuzzo, R. G.; Whitesides, G. M. *Chem. Rev.* **2005**, *105*, 1103–1169.
- Schlichte, K.; Kratzke, T.; Kaskel, S. *Microporous Mesoporous Mater.* **2004**, *73*, 81–88.
- Alaerts, L.; Seguin, E.; Poelman, H.; Thibault-Starzyk, F.; Jacobs, P. A.; De Vos, D. E. *Chem.—Eur. J.* **2006**, *12*, 7353–7363.
- Krawiec, P.; Kramer, M.; Sabo, M.; Kunschke, R.; Froede, H.; Kaskel, S. *Adv. Eng. Mater.* **2006**, *8*, 293–296.
- Wang, H.; Chen, S.; Li, L.; Jiang, S. *Langmuir* **2005**, *21*, 2633–2636.
- Ulman, A. *An Introduction to Ultrathin Organic Films: From Langmuir-Blodgett to Self-Assembly*; Academic Press: San Diego, CA, 1991.

JA0701208